Arch. Metall. Mater. **66** (2021), 3, 755-758

DOI: 10.24425/amm.2021.136375

SUNG YEON RYU[1], HEE JU YUN[1], MIN HWAN LEE[2], BYUNG JOON CHOI[1*]

# GROWTH TEMPERATURE EFFECT OF ATOMIC-LAYER-DEPOSITED $GdO_x$ FILMS

Gadolinium oxide ($Gd_2O_3$) is one of the lanthanide rare-earth oxides, which has been extensively studied due to its versatile functionalities, such as a high permittivity, reactivity with moisture, and ionic conductivity, etc. In this work, $GdO_x$ thin film was grown by atomic layer deposition using cyclopentadienyl (Cp)-based Gd precursor and water. As-grown $GdO_x$ film was amorphous and had a sub-stoichiometric (x ~ 1.2) composition with a uniform elemental depth profile. ~3 nm-thick $GdO_x$ thin film could modify the hydrophilic Si substrate into hydrophobic surface with water wetting angle of 70°. Wetting and electrical test revealed that the growth temperature affects the hydrophobicity and electrical strength of the as-grown $GdO_x$ film.

*Keywords:* gadolinium oxide ($Gd_2O_3$), rare-earth oxide, atomic layer deposition, hydrophobicity, electrical property

## 1. Introduction

Rare-earth oxides have attracted ever increasing attention for applications in various fields of microelectronics and electrochemical energy conversion [1,2]. Their metal atoms have a distinctive electronic structure in the series; the unfilled 4f orbitals are shielded by the fully occupied electrons in the outer shell [3,4]. As a result, the value of the oxidation states progressively changes along the series, which significantly affects their electronic property and chemical reactivity.

Among the various rare-earth oxides, gadolinium oxide ($Gd_2O_3$) and its derivatives have been particularly interesting for micro- and optoelectronic applications due to their versatile functionalities [5,6]. Govindarajan et al. reported that HfGdO-based metal-oxide-semiconductor capacitors exhibited an improvement of low leakage current and increased permittivity up to 28 [7]. Their essential finding was that rare-earth element could stabilize the higher permittivity tetragonal phase. Kim et al. addressed the reduced interface trap density in $Gd_2O_3$ dielectric layer formed on n-type GaN substrate; as such, much improved rectifying characteristics were observed in GaN Schottky diode [8].

Atomic layer deposition (ALD) can be the key process for the preparation of rare-earth oxide including $Gd_2O_3$ [4,6,8-11]. It enables outstanding uniformity over the full wafer-scale and excellent conformality at the atomic scale. The challenge of ALD in rare-earth oxide is the strong hygroscopic nature of rare-earth oxide: highly sensitive to the moisture [6]. Such a reactivity may lead to parasitic chemical vapor deposition (CVD) reaction due to the adsorbed $H_2O$ and hydroxyl ($OH^-$) group.

In this study, we prepared the $GdO_x$ thin films on a variety of substrates by using a thermal ALD process. Chemical composition and microstructure of the films were characterized, where the films were grown at the substrate temperature of 200, 225, and 250°C. Hydrophobicity and electrical properties of ALD-grown $GdO_x$ films were investigated.

## 2. Experimental

The $GdO_x$ films was grown by conventional traveling-wave-type ALD reactor (Atomic Classic, CN-1 Co., Korea). Thermal ALD was processed with $(RCp)_2Gd(L)$ (Air Liquide, USA) as the Gd precursor and $H_2O$ as the oxidant [8]. Canisters of $(RCp)_2Gd(L)$ and water were kept at 110 and 25°C, respectively. The substrate temperature was varied from 200 to 300°C. Nitrogen (high purity of 99.9999%) gas was used to control the working pressure as well as the purging gas. ALD growth was performed on the various substrate surface: Si, $SiO_2$ on Si, glass, and TiN. The pulse sequence for the $GdO_x$ film was composed as follows: Gd source feeding (2s) – $N_2$ purge (120s) – $H_2O$ feeding (1s) – $N_2$ purge (30s).

Auger electron spectroscopy (AES: PHI 700, ULVAC-PHI, Japan) were used for the analysis of depth profile of a chemical composition. To observe the microstructure of ALD-grown

[1] SEOUL NATIONAL UNIVERSITY OF SCIENCE AND TECHNOLOGY, DEPARTMENT OF MATERIAL SCIENCE AND ENGINEERING, SEOUL 01811, KOREA
[2] UNIVERSITY OF CALIFORNIA MERCED, DEPARTMENT OF MECHANICAL ENGINEERING, MERCED, CALIFORNIA, USA

* Corresponding author: bjchoi@seoultech.ac.kr

$GdO_x$ film on the substrate, cross-sections were prepared using a focused ion beam (FIB: Nova 200, FRI, Netherlands), and imaging was performed using a high-resolution transmission electron microscopy (HRTEM: JEM-2100F, JEOL, Japan). Optical transmittance and band gap energy of the film was examined by UV-Visible spectrometer (UV-Vis: Lambda 35, PerkinElmer, USA). Contact-angle of water droplet on the film surface was measured by contact-angle goniometer (CAM-200, KSV, Finland).

To verify the electrical properties, devices were fabricated using Pt (100 nm) as a top electrode and TiN as a bottom electrode on $SiO_2$/Si substrate. After growing 4-nm-thick $GdO_x$ thin film, 100-nm-thick Pt layer was deposited by sputtering and photolithographically patterned for a square-shaped top electrode with a length of 50 μm. Semiconductor parameter analyzer (HP-4155A, AGILENT, USA) was used to analyze electrical characteristics of $GdO_x$ thin films by measuring current-voltage (I-V) hysteresis at room temperature.

## 3. Results and discussion

Figure 1 (a) shows the ALD-grown film thickness as a function of the number of ALD cycles at the various temperatures. Film thicknesses grown at 200 and 250°C exhibit slightly different offset but the similar slope. On the contrary, much retarded growth was observed at 275°C. From the slope of linear fitting in the points, growth rate of $GdO_x$ film could be estimated as shown in Figure 1 (b). ALD window – temperature range having a constant growth rate – of $GdO_x$ film seems to be the range of 200 to 250°C, and the growth rate in the ALD window was around 0.1 nm/cycle. Whereas, the decreased growth rate above the growth temperature at 275°C was observed; the reason of such a decreased growth rate was not clear at this moment. Desorption of the precursor or sublimation of the film could be the possible reason of it. Therefore, $GdO_x$ films grown at 200, 225, and 250°C within the ALD window were mainly characterized to reveal those chemical and physical properties depending on the growth temperature.

Depth profile of elemental concentration of the $GdO_x$ films was characterized by AES analysis. Figure 2 (a) and (b) compare the depth profiles of as-grown 7-nm-thick $GdO_x$ films at 200 and 250°C. Uniform depth profiles of Gd and O are observed in the figure. Both results exhibited that composition of $GdO_x$ films were slightly sub-stoichiometric (O/Gd ~ 0.54/0.45 = 1.2); reduced phase (x < 1.5) was deposited rather than stoichiometric $Gd_2O_3$. Similar elemental profile was observed in the film

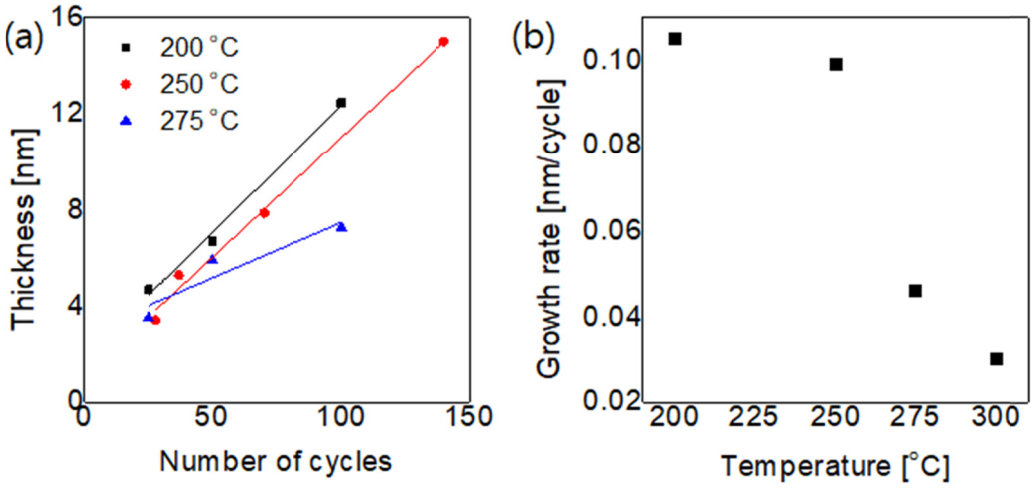


Fig. 1. (a) $GdO_x$ film thickness as a function of the number of ALD cycles (b) the growth rate of $GdO_x$ film according to the growth temperature

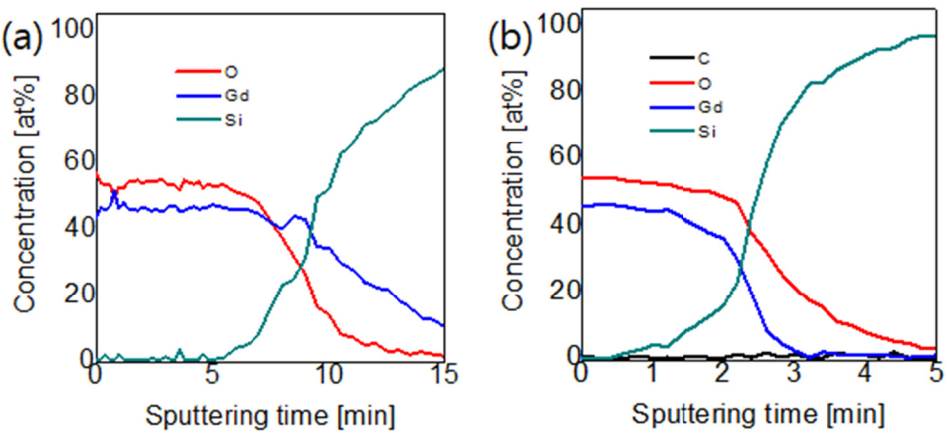


Fig. 2. AES depth profile of atomic concentration in the $GdO_x$ film grown at (a) 200 and (b) 250°C

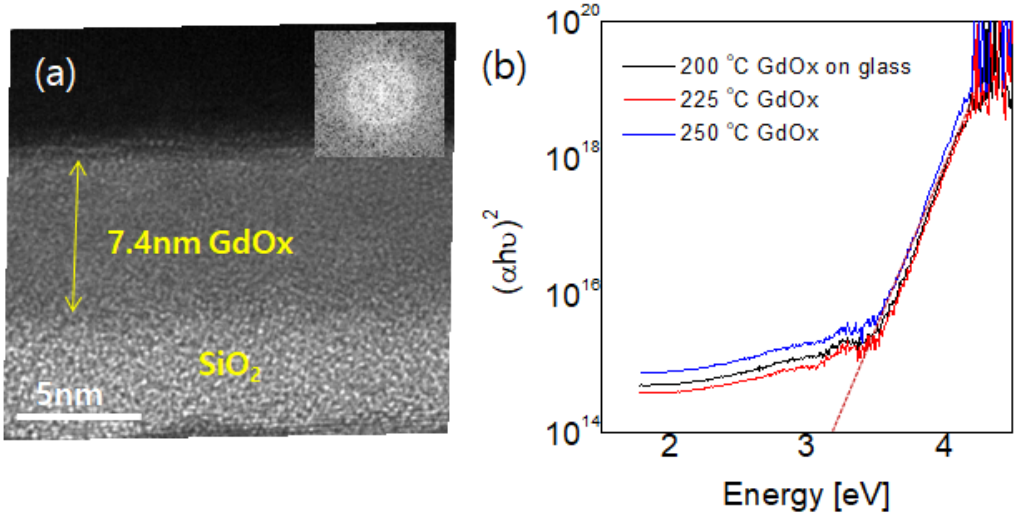


Fig. 3. (a) Cross-sectional TEM image of the $GdO_x$ film grown on $SiO_2$ at 250°C (inset: electron diffraction pattern) (b) Tauc plot of direct band gap energy of the $GdO_x$ film grown on glass at 200, 225, and 250°C

grown at 225°C. Slight difference in the depth profile near Si interface was attributed to the different sputtering rate during the film analysis.

Figure 3 (a) shows the cross-sectional TEM image of the as-deposited 7.4-nm-thick $GdO_x$ film at 250°C. No crystalline lattice fringe can be seen in the figure. Inset figure of electron diffraction also reveals the amorphous nature of ALD-grown $GdO_x$ film. Therefore, it appears that microstructure of $GdO_x$ film grown in the ALD window (200-250°C) is an amorphous phase.

Optical band gap of $GdO_x$ films were characterized by their transmittance upon the UV and visible light (200-900 nm). The transmittance of ~3-nm-thick $GdO_x$ films grown on glass substrate was measured by UV-Vis spectrometer. Optical band gap energy can be calculated by absorption coefficient α following Tauc method [12]. The optical band gap energy can be estimated the intercept of x-axis with the linear-fitted line as shown in Fig. 3(b). As a result, only ~3.3 eV of band gap energy was outcome by the linear fitting. However, this value could not be the band gap energy of $GdO_x$ film because it has been reported that the band gap energy of $GdO_x$ film is higher than 5.7 eV and hardly reported as below 5.37 eV in the literature [13,14]. Therefore, we believe that this low band gap energy was given by the interfacial layer between the $GdO_x$ film and the glass substrate rather than $GdO_x$ film itself.

Water contact-angle was evaluated for the hydrophobicity of ALD-grown $GdO_x$ films. Film thickness was ~3 nm grown at 200, 225, and 250°C on Si. As-grown $GdO_x$ film at 250°C was annealed under $O_2$ at 400°C for 20 min. Wetting angle of Si substrate as a reference was ~38°; on the contrary, those of $GdO_x$ films were increased with increasing the growth temperature. $GdO_x$ film grown at 250°C showed the highest hydrophobicity with water contact-angle as high as 70°. After annealing at 400°C, however, hydrophobicity was degraded; contact-angle was slightly decreased to 60°. This decrement of wetting angle is attributed to the hygroscopic nature of $GdO_x$ film. Hygroscopic materials tend to absorb moisture so that large amount of hydroxyl group ($OH^-$) is produced on surfaces [4]. Hydrophobic surface of as-grown $GdO_x$ film may be turned into less hydrophobic after annealing in $O_2$ atmosphere.

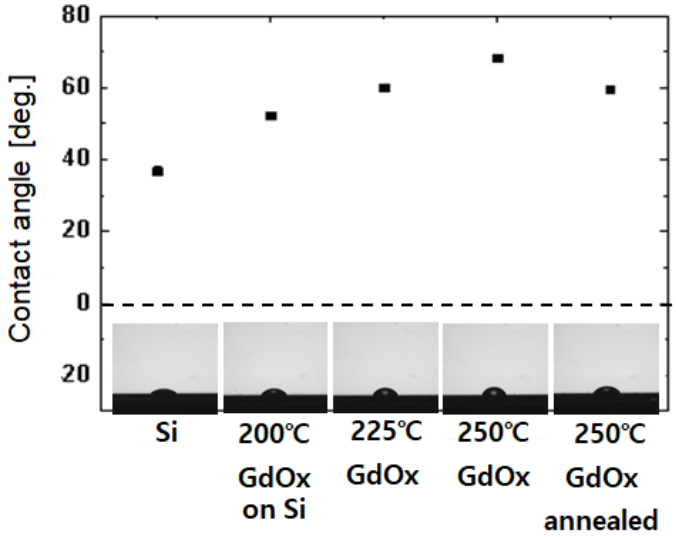


Fig. 4. Contact-angle of water droplet on Si and ~3-nm-thick $GdO_x$ film deposited on Si at 200, 225, and 250°C. $GdO_x$ film was annealed at 400°C for 20 min

To compare the electrical properties of the devices having Pt/$GdO_x$/TiN stack, I-V characterization was performed. ~4-nm-thick $GdO_x$ films grown at 200, 225, and 250°C was employed for this examination. Figure 5(a) reveals the cross-sectional TEM image of the device with $GdO_x$ film at 250°C formed on both TiN contact-hole and surrounded inter-dielectric layer. Figure 5(b) represents the I-V curves and their soft-breakdown behaviors of the 3 devices. The pristine devices were remained in the insulating states; resistance values read at –0.2 V were 75 kΩ, 81 kΩ, and 8.9 MΩ for the device with the films grown at 200, 225, and 250°C, respectively. Therefore, it appears that

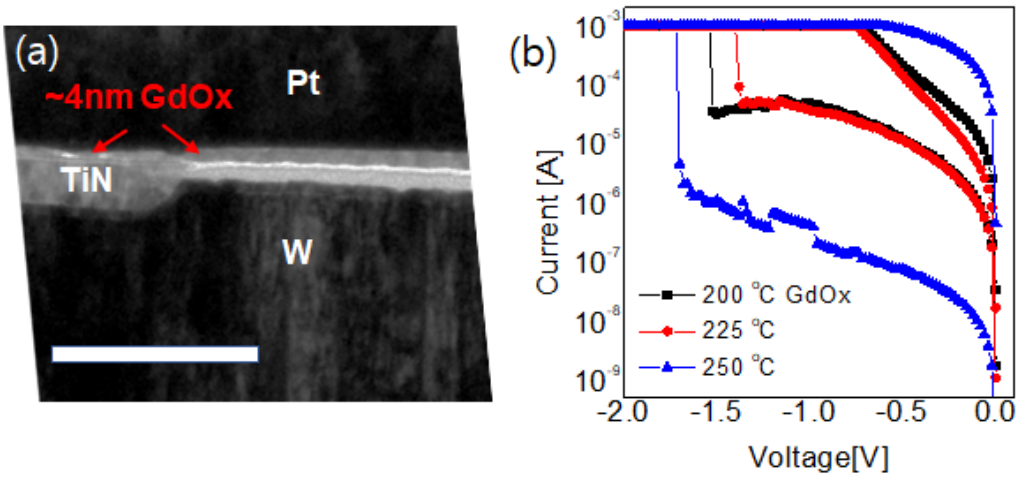


Fig. 5. (a) Cross-sectional TEM image of the device (scale bar: 100 nm) (b) I-V curves of Pt/$GdO_x$/TiN device with the different growth temperature

the initial resistance is increased more than 100 times along with the growth temperature between 225 and 250°C. Initially insulating state was transitioned to the conducting state by soft-breakdown process. The voltage that soft-breakdown happened was –1.52, –1.36, and –1.70 V for the device fabricated at 200, 225, and 250°C, respectively. Soft-breakdown voltage seems to be related to the initial resistance; more insulating $GdO_x$ film grown at 250°C has higher soft-breakdown voltage. Although ALD-grown $GdO_x$ film in this experimental range has mainly amorphous microstructure, denser and less defective film is likely grown at the elevated temperature.

## 4. Conclusions

Thermal ALD could grow the $GdO_x$ thin film at a temperature of 200-250°C by using $(RCp)_2Gd(L)$ and water as Gd precursor and oxidant gas. Film growth rate was around 0.1 nm/cycle. Uniform Gd and O concentration in the film was observed, but sub-stoichiometric $GdO_x$ (x ~ 1.2) film was proven by AES depth profile analysis. The film grown on $SiO_2$ at 250°C was amorphous. It is note-worthy that hydrophobic surface modification was exhibited by 3-nm-thick $GdO_x$ thin film grown on Si. Electrical test revealed that $GdO_x$ film grown at 250°C showed the more insulating and stronger to breakdown field. Most hydrophobic and insulating $GdO_x$ film was grown at 250°C. Therefore, it is believed that growth temperature affects the functionality of $GdO_x$ film, such as hydrophobicity and electrical property.

### Acknowledgments

This study was financially supported by Seoul National University of Science & Technology.

## REFERENCES

[1] C. Wiemer, L. Lamagna, M. Fanciulli, Semiconductor Science and Technology **27**, 074013 (2012).
[2] A. Karimaghaloo, J. Koo, H. sen Kang, S.A. Song, J.H. Shim, M.H. Lee, International Journal of Precision Engineering and Manufacturing - Green Technology **6**, 611 (2019).
[3] G. Azimi, R. Dhiman, H.M. Kwon, A.T. Paxson, K.K. Varanasi, Nature Materials **12**, 315 (2013).
[4] I.K. Oh, K. Kim, Z. Lee, K.Y. Ko, C.W. Lee, S.J. Lee, J.M. Myung, C. Lansalot-Matras, W. Noh, C. Dussarrat, H. Kim, H.B.R. Lee, Chemistry of Materials **27**, 148 (2015).
[5] M. Leskelä, K. Kukli, M. Ritala, Journal of Alloys and Compounds **418**, 27 (2006).
[6] J.H. Han, A. Delabie, A. Franquet, T. Conard, S. van Elshocht, C. Adelmann, Chemical Vapor Deposition **21**, 352 (2015).
[7] S. Govindarajan, T.S. Böscke, P. Sivasubramani, P.D. Kirsch, B.H. Lee, H.H. Tseng, R. Jammy, U. Schröder, S. Ramanathan, B.E. Gnade, Applied Physics Letters **91**, 062906 (2007).
[8] H. Kim, H.J. Yun, B.J. Choi, RSC Advances **8**, 42390 (2018).
[9] J.H. Shim, G.D. Han, H.J. Choi, Y. Kim, S. Xu, J. An, Y.B. Kim, T. Graf, T.D. Schladt, T.M. Gür, F.B. Prinz, International Journal of Precision Engineering and Manufacturing - Green Technology **6**, 629 (2019).
[10] K. Xu, R. Ranjith, A. Laha, H. Parala, A.P. Milanov, R.A. Fischer, E. Bugiel, J. Feydt, S. Irsen, T. Toader, C. Bock, D. Rogalla, H.J. Osten, U. Kunze, A. Devi, Chemistry of Materials **24**, 651 (2012).
[11] C. Adelmann, H. Tielens, D. Dewulf, A. Hardy, D. Pierreux, J. Swerts, E. Rosseel, X. Shi, M.K. van Bael, J.A. Kittl, S. van Elshocht, Journal of The Electrochemical Society **157**, G105 (2010).
[12] D. Kim, D. Ha Kim, D.H. Riu, B.J. Choi, Archives of Metallurgy and Materials **63**, 1061 (2018).
[13] M. Mishra, P. Kuppusami, S. Ramya, V. Ganesan, A. Singh, R. Thirumurugesan, E. Mohandas, Surface and Coatings Technology **262**, 56 (2015).
[14] N.K. Sahoo, M. Senthilkumar, S. Thakur, D. Bhattacharyya, Applied Surface Science **200**, 219 (2002).